Scripta Materialia 141 (2017) 85–88

Contents lists available at ScienceDirect

Scripta Materialia

journal homepage: www.elsevier.com/locate/scriptamat

Regular article

# Non-dislocation-mediated basal stacking faults inside $\{10\bar{1}1\}$ twins

Qi Sun [a], Qiwei Zhang [b], Bin Li [b,*], Xiyan Zhang [a,*], Li Tan [a], Qing Liu [a]

[a] School of Materials Science and Engineering, Chongqing University, People's Republic of China
[b] Department of Chemical and Materials Engineering, University of Nevada, Reno, NV 89557, USA

ARTICLE INFO

*Article history:*
Received 11 May 2017
Received in revised form 26 July 2017
Accepted 30 July 2017
Available online xxxx

*Keywords:*
Stacking faults
Hexagonal close-packed metals
Twin
Transmission electron microscopy

ABSTRACT

Anomalous basal stacking faults have frequently been observed inside $\{10\bar{1}2\}$ twins in deformed hcp metals. In this work, we report transmission electron microscopy observation of basal stacking faults inside $\{10\bar{1}1\}$ twins. These stacking faults present similar characteristics to those inside $\{10\bar{1}2\}$ twins. To reveal the formation mechanism, we performed atomistic simulations. The results show that the stacking faults are not mediated by partial dislocations. Lattice transformation analysis based on classical twinning theory shows that very large atomic shuffles (~0.16 nm) perpendicular to the twinning shear are required for twinning and responsible for the formation of these stacking faults.



Stacking faults (SFs), as a type of planar defects in crystalline metals, are mostly related to the glide of partial dislocations. They are often observed in plastically deformed metals [1] or irradiated materials [2]. Energetically, a partial dislocation is more favorable over a full dislocation due to lower energy barrier for gliding on close-packed crystallographic planes. As a result, an SF is formed behind a leading partial. Then a trailing partial is formed to erase the SF. Thus, the balance between the stacking fault energy (SFE) and the mechanical energy of the two partial dislocations determines the equilibrium width of the SF [1]. In general, the equilibrium width $d$ is inversely proportional to the SFE [1].

For hexagonal close-packed (hcp) metals, although the basal SFE is relatively low, the equilibrium width of a basal SF generated by Shockley partials is only 1–3 nm [3], which is uneasy to be identified by the conventional transmission electron microscopy (TEM). However, several TEM studies on the microstructure of deformed hcp metals suggested that a special type of basal SF with a width that is two or three orders of magnitude larger than the equilibrium width of basal SF can be formed [4–7], especially inside $\{10\bar{1}2\}$ twins [8–12]. Experimental and simulation studies have been carried out to understand the mechanism of such anomalous SFs [4–11]. Song and Gray [8–10] suggested that the formation of such anomalous SFs inside $\{10\bar{1}2\}$ twins is related to the movements of a large number of atoms involved in twin growth rather than partial dislocations. They defined these SFs as "partial stacking faults" because only every other basal plane on one side of an SF are displaced, which differs from $I_1$ (produced by Frank partials) and $I_2$ (produced by Shockley partials) SFs. Zhang and Li [11] performed TEM observations and atomistic simulations of basal SFs, and their results showed that the formation of the anomalous SFs inside $\{10\bar{1}2\}$ twins is related to incoherent twin boundary (TB) migration involving large atomic shuffles. These SFs may interact with dislocation slip and influence the mechanical property of hcp materials [11,13].

In addition to $\{10\bar{1}2\}$ twinning, $\{10\bar{1}1\}$ twinning has been observed in hcp metals [14,15]. This twinning mode is usually activated at higher stresses and have been related to fracture during plastic deformation [16,17]. Thus, interesting questions arise: Can such anomalous basal SFs also be formed inside $\{10\bar{1}1\}$ twins? If yes, what is the mechanism responsible for the formation? Are there similarities to those basal SFs inside $\{10\bar{1}2\}$ twins? To date, there have not been direct experimental studies on basal SFs inside $\{10\bar{1}1\}$ twins.

The purpose of the current work is to carefully examine basal SFs inside $\{10\bar{1}1\}$ twins in deformed hcp metals, by performing TEM observations and atomistic simulations. Indeed, high density basal SFs were observed. A possible mechanism responsible for the formation of such SFs is proposed.

Two hcp metals, Mg-3%Al-1%Zn (AZ31) magnesium alloy and pure cobalt, were investigated in this study. Tension samples were cut from the hot-rolled AZ31 magnesium alloy sheet with strong basal texture, and tensile deformation was performed parallel to the rolling direction (RD) at room temperature at a quasi-static strain rate of $10^{-3}\ s^{-1}$ until fracture. TEM samples were taken at the vicinity of the fracture surface by electrical discharge machining (EDM). Then the samples were thinned by grinding followed by low temperature ion milling. Subsequently, the TEM observations were carried out on a JEM-2100 electron

* Corresponding authors.
*E-mail addresses:* binl@unr.edu (B. Li), kehen888@163.com (X. Zhang).

http://dx.doi.org/10.1016/j.scriptamat.2017.07.036

microscopy with a voltage of 200 kV. Microstructure of dynamically deformed Co samples (strain rate ~ $10^3\ s^{-1}$) was also examined by TEM and the experimental details can be found in [18].

To understand the deformation mechanisms, we performed atomistic simulation of tensile deformation of single crystal Mg using an Embedded Atom Method (EAM) [19,20] type potential for Mg [21]. Recently, Modified EAM (MEAM) [22] potentials for Mg have been developed by Wu and Curtin [23] for better accuracy of SFE. The system contains ~300,000 atoms with dimensions of 26 × 17 × 16 nm. The system temperature was maintained at 10 K. Free surfaces were applied to all dimensions. The system was relaxed for 10,000 time steps (30 ps) before straining. A tensile load was applied along the $1\bar{2}10$ by moving one end of the box at a displacement rate of $a_0/10000$ ($a_0 = 0.321$ nm is the lattice parameter of Mg) per time step, corresponding to a strain rate of $8.0 \times 10^8\ s^{-1}$ while the other end was fixed. The time step size was 3.0 fs.

Fig. 1(a) displays a typical bright-field TEM micrograph of a $\{10\bar{1}1\}$ twin in the deformed AZ31 at a relatively low magnification. The electron beam is nearly parallel to the $1\bar{2}10$ zone axis. Selected area electron diffraction (SAED) was performed at location 1 which comprises both the parent and the twin. The corresponding SAED pattern is shown in Fig. 1(b), which clearly indicates the $\{10\bar{1}1\}$ twin orientation relationship. Inside the twin (Fig. 1(a)), a high density of basal SFs can be observed. These SFs may cross the whole twin with a width more than 500 nm. These basal SFs are similar to those basal SFs observed inside $\{10\bar{1}2\}$ twin [11]. SAED was also performed at location 2 (see Fig. 1(a)) which is inside the twin, and the diffraction pattern is shown in Fig. 1(c). As indicated by the arrow, streaking along the [0001] direction (i.e. the *c*-axis) can be observed. This indicates that these SFs are indeed on the (0002) basal planes of the twin. It is worth noting that the width of these basal SFs is two to three orders of magnitude wider than the equilibrium width (1–3 nm) of the basal SFs produced by Shockley partials in magnesium alloy [3]. These basal SFs can cross the whole twin with both ends anchored at the opposite TBs, or terminate inside the twin, similar to those basal SFs observed inside $\{10\bar{1}2\}$ twins [11].

Basal SFs were not only observed in deformed Mg, but also in deformed cobalt inside $\{10\bar{1}1\}$ twins, as shown in Fig. 2(a). The electron beam is along the $1\bar{2}10$ zone axis. At a relatively low magnification, diffraction contrast of basal SFs can be observed as straight lines that are parallel to the trace of the basal plane. The diffraction pattern of the twins taken at the twinning boundary is shown in the inset. The basal SFs may cross the whole twin as well, with a width over hundreds of nanometers. Fig. 2(b) displays an HRTEM micrograph near the TB. It can be observed that one end of the basal SFs are anchored at the TB.

The above TEM and HRTEM observations indicate that anomalous basal SFs can, indeed, be generated inside $\{10\bar{1}1\}$ deformation twins in hcp Mg and Co. These basal SFs have similar characteristics to those inside $\{10\bar{1}2\}$ twins. In the following, we present atomistic simulation results to resolve the mechanism responsible for the formation of these anomalous basal SFs.

Under the tensile strain, $\{10\bar{1}1\}$ twinning was activated, as shown in Fig. 3(a) and (b). Notably, during twin nucleation and growth, a number of anomalous basal SFs were formed inside the $\{10\bar{1}1\}$ twin, as shown in Fig. 3(a). In these plots, common neighbor analysis [24] was used to display structures that deviate from the ideal hcp structure which is represented by the red atoms. The TBs, which are denoted by the gray atoms, coincide with the $\{10\bar{1}1\}$ plane. The SFs are denoted by the green atoms which lie on the basal plane of the twin. It can be seen that the two ends of the SFs are connected to the TBs, thus these SFs cross the whole $\{10\bar{1}1\}$ twin. As the tensile strain increases, the SFs grow wider as the TBs migrate and the twin thickens. During twin growth, both ends of the SFs remain anchored at the TBs, as shown in Fig. 3(b). As a result, these basal SFs always appear across the whole twin as the width increases. At the intersections of the SFs and the TBs, one-layer steps can be observed. The two-layer steps are partial zonal twinning dislocations [16,25] which can glide over the one-layer steps without interaction. It can also be seen that the basal SFs may terminate inside the $\{10\bar{1}1\}$ twin while the other end is connected to the TB. This scenario occurs when a defect is generated inside the twin and the anomalous basal SF is actually terminated at the defect. Our simulation results are highly consistent with our TEM observations.

The anomalous basal SFs shown in Figs. 3 and 4 differ from those basal SFs created by the glide of Shockley partial dislocations in that a

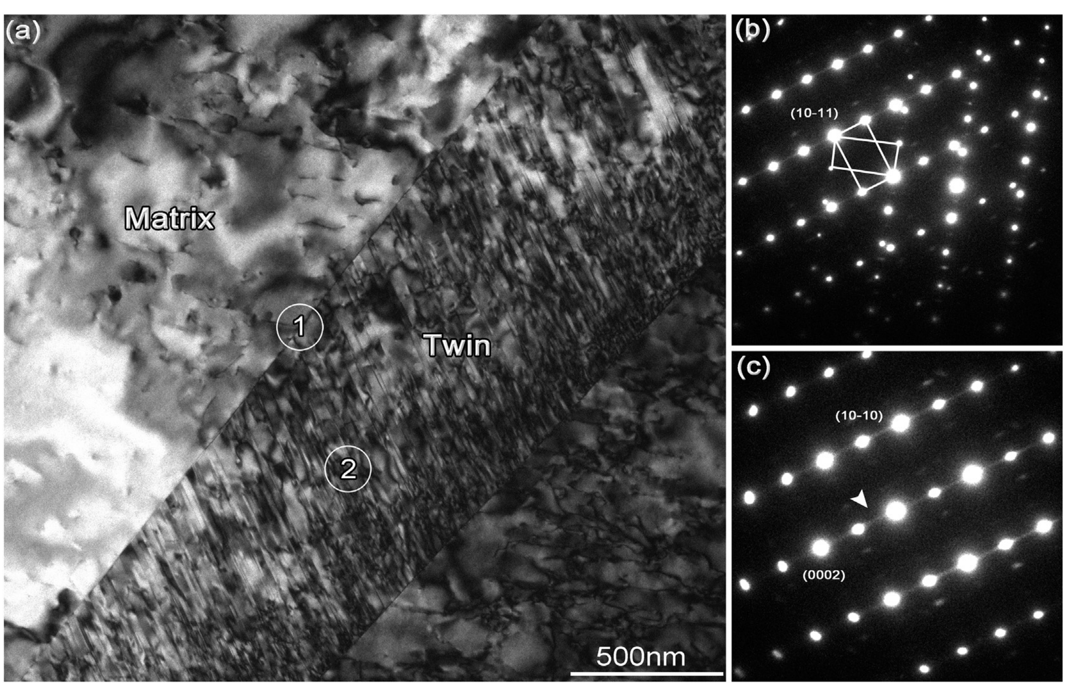


**Fig. 1.** (a) A bright-field TEM micrograph shows high density of basal stacking faults inside a $\{10\bar{1}1\}$ deformation twin in a deformed AZ31 magnesium alloy. The electron beam is nearly parallel to the $1\bar{2}10$ zone axis. (b) Selected area electron diffraction pattern taken from the circled region 1 in (a), indicating the $\{10\bar{1}1\}$ twin orientation relationship. (c) A diffraction pattern for the circled region 2 in (a). The presence of streaking indicated by the white arrow indicates that the stacking faults are on the (0002) basal plane.

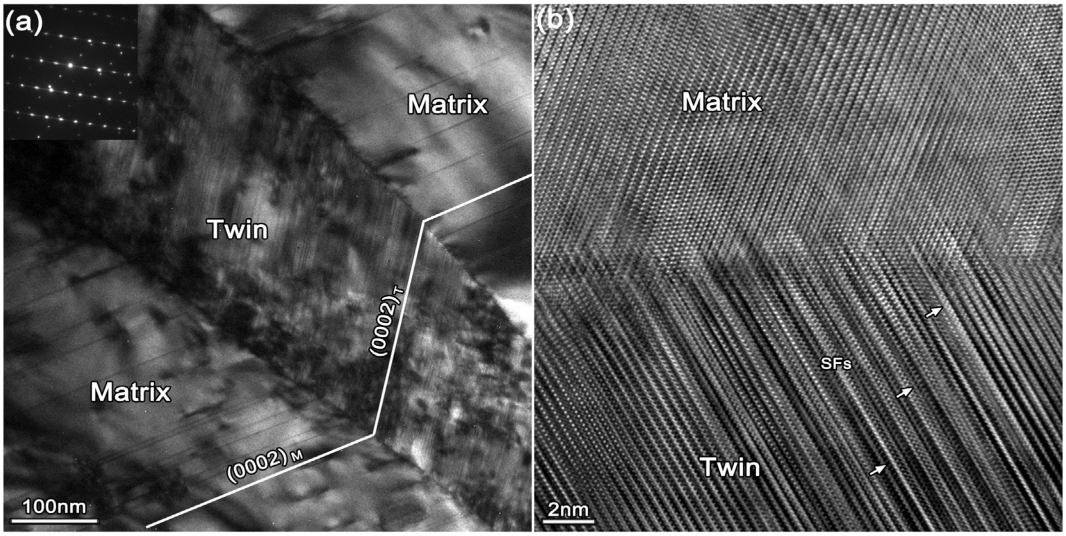


**Fig. 2.** (a) A bright-field TEM micrograph shows high density of basal stacking faults inside a $\{10\bar{1}1\}$ twin in deformed cobalt. The selected area electron diffraction pattern (the inset) was taken from the twinning boundary (zone axis $1\bar{2}10$). The basal planes of twin and matrix are indicated by the white lines. (b) HRTEM image shows the region near the twinning boundary in (a). Basal stacking faults inside the $\{10\bar{1}1\}$ twin are indicated by the arrows.

two-layer fcc stacking (…*ABC*…) is generated near the SFs. In contrast, a three-layer fcc stacking (…*ABCA*…) is generated near an SF by a Shockley partial and a global displacement vector can be defined [5,26]. Anomalous basal SFs have frequently been observed inside $\{10\bar{1}2\}$ twins both in experiment and simulation studies of hcp metals [8–11]. Zhang et al. [11] showed that such SFs are closely related to incoherent TB migration. Li and Zhang [27] has recently argued based on shuffling theory that $\{10\bar{1}2\}$ twinning mode is accomplished solely by atomic shuffling and no shear is involved [28]. For Mg, the maximum magnitude of atomic shuffles can be as large as ~0.1 nm [27]. Such large shuffles may cause atoms to land on faulted positions during incoherent TB migration [11]. Therefore, anomalous basal SFs are closely related to large atomic shuffles that are required for specific twinning modes.

Detailed information of atomic shuffling for $\{10\bar{1}1\}$ twinning, however, is not available in the literature. Bilby and Crocker [29], Christian and Mahajan [16] schematically showed some atomic shuffles in their works. But their analysis is incomplete. In the following, we analyze the shuffling based on lattice correspondence which is a central feature in deformation twinning.

According to the classical twinning theory [16,29], a plane of the parent is transformed to a plane of the twin, and a one-to-one lattice correspondence can be uniquely established for each twinning mode [30]. Li and Ma [25] showed that in $\{10\bar{1}1\}$ twinning, the basal plane, i.e. $(0002)_P$ of the parent is transformed to the pyramidal plane, i.e. $\{10\bar{1}\bar{1}\}_T$ of the twin. Such a transformation is consistent with the calculations based on the classical twinning theory [30]. Thus, we can analyze the shear and shuffle in detail by analyzing the lattice transformation.

Fig. 4 shows the structure of a $\{10\bar{1}1\}$ plane. The viewing direction is along the normal direction of the $\{10\bar{1}1\}$ plane. This pyramidal plane has a double-layer structure in which atoms are located on two slightly separate planes. The double-layer structure is represented by the red and the blue atoms. On top of the $\{10\bar{1}1\}$ plane, a hexagonal basal plane (represented by the hollow green atoms) is superimposed. At the bottom layer, the atoms of the two planes perfectly coincide along the zone

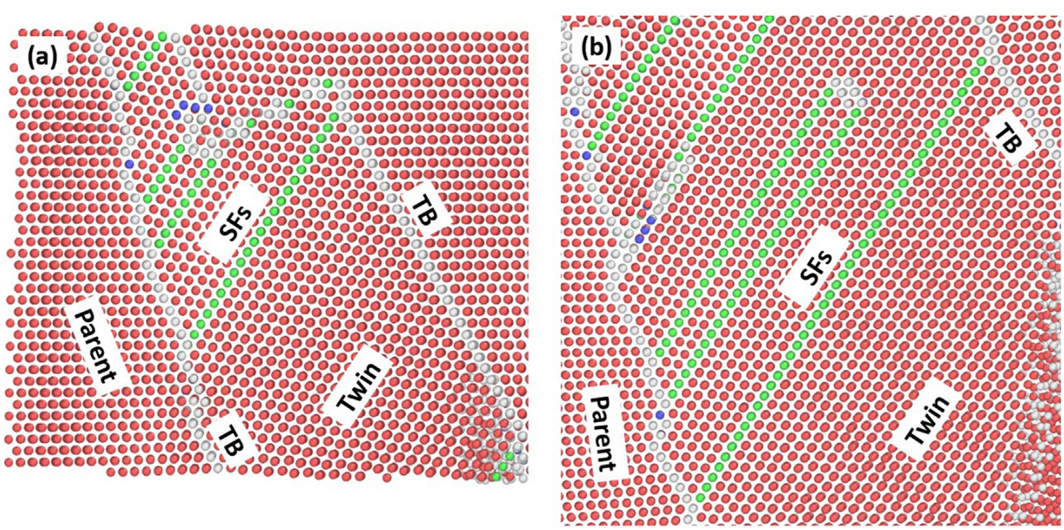


**Fig. 3.** Atomistic simulations of basal stacking faults across a $\{10\bar{1}1\}$ twin. (a) Basal stacking faults (in green) inside a $\{10\bar{1}1\}$ twin. The twin boundaries are colored in gray, and the red atoms are situated in perfect HCP lattice positions. (b) As twinning proceeds and the TB (in gray) migrates, the basal SFs (in green) grow wider with both ends anchored at the TBs. Some of the SFs may terminate inside the $\{10\bar{1}1\}$ twin. (For interpretation of the references to color in this figure legend, the reader is referred to the web version of this article.)

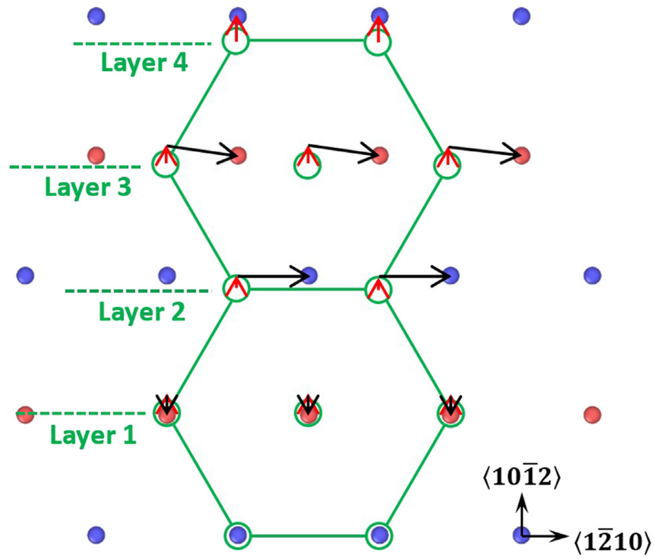


**Fig. 4.** Transformation of a (0002) basal plane to a {10$\bar{1}$1} plane during {10$\bar{1}$1} twinning. The double-layer structure of a {10$\bar{1}\bar{1}$} plane is shown by the blue and red atoms which are actually located on two slightly separate planes. A basal plane (denoted by the hollow green circles) is superimposed on top of the {10$\bar{1}\bar{1}$} plane to show that shuffles as large as $\frac{1}{2}a_0$ ($a_0$ is the lattice parameter of Mg, i.e. 0.321 nm) are required for atoms at layer 2 and 3 during twinning. The red arrows indicate the shear and the black arrows indicate the shuffles. (For interpretation of the references to color in this figure legend, the reader is referred to the web version of this article.)

axis 1$\bar{2}$10. At layer 4, the green atoms are sheared directly to the twin positions without the need of shuffling, and the shear is represented by the red arrows. Thus, the twinning dislocation is a four-layer or a two-layer zonal dislocation [16]. Because a twinning shear is an affine shear [16], layer 1, 2 and 3 should experience the same homogeneous shear (indicated by the red arrows). The magnitude of the red arrows at individual layers is proportional to the distance from the bottom layer. At layer 1, the green atoms are sheared along the twinning direction, then they must slightly shuffle backwards to reach the twin positions denoted by the red atoms. At layer 2, the green atoms are first sheared along the twinning direction, then they must shuffle by a large distance $\frac{1}{2}a_0 \approx 0.1$ 6 nm ($a_0$ is the lattice parameter of Mg, which equals 0.321 nm) to reach the twin positions denoted by the blue atoms. The magnitude of this shuffle is about five times the magnitude of the elementary twinning dislocation on each twinning plane. It is worth noting that the shuffling direction is nearly perpendicular to the twinning direction. A similar scenario applies to the green atoms at layer 3, but a component against the twinning direction has to be involved in the shuffling.

The analysis in Fig. 4 clearly indicates that very large and complex shuffles are required to complete the lattice transformation. However, at layer 2 and 3, the shuffling direction indicated by the black arrows is not the only option. If the green atoms at layer 2 or 3 shuffle opposite to the black arrows, a basal SF will be created inside the {10$\bar{1}$1} twin. This could happen as a result of disruptions that lead to atoms landing on the faulted positions. Basal SFs were also reported by Fan and El-Awady [12] in their atomistic simulations. Ostapovets and Serra [31] observed similar SFs in their simulation of {10$\bar{1}$1} twinning and they showed that a Burgers circuit can be drawn around the one-layer steps. However, according to Song and Gray [8], only half of the atoms on one side of an SF are displaced and no global displacement vector can be defined.

To conclude, high density, anomalous basal SFs inside {10$\bar{1}$1} twins in deformed hcp metals were observed by TEM. These basal SFs may cross a whole twin and grow as TBs migrate and present similar characteristics to basal SFs inside {10$\bar{1}$2} twins. Atomistic simulations reveal that these basal SFs are not mediated by partial dislocations. Lattice correspondence analysis shows that very large atomic shuffles (~0.16 nm) in the direction nearly perpendicular to the twinning shear are required for {10$\bar{1}$1} twinning. Such large shuffles may cause atoms to land on faulted positions during twinning, leading to basal SFs inside {10$\bar{1}$1} twins without the glide of partial dislocations.

## Acknowledgements

Q. Sun and X.Y. Zhang acknowledge the support from the National Natural Science Foundation of China (Grant No. 51271208, 51671040, 50890170 and 51421001) and the Basic Research of China (No. 2010CB631004). B. Li gratefully thanks the support from U.S. National Science Foundation (CMMI-1635088).

## References

[1] J.P. Hirth, J. Lothe, Theory of Dislocation, 2nd ed. John Wiley & Sons, New York, 1982.
[2] Y. Huo, X.T. Zhu, A. Li, Z.G. Wang, L.M. Wang, Acta Mater. 52 (2004) 2683.
[3] J.A. Yasi, L.G. Hector Jr., D.R. Trinkle, Acta Mater. 60 (2012) 2350–2358.
[4] S.R. Agnew, J.A. Horton, M.H. Yoo, Metall. Mater. Trans. A 33 (2002) 851–858.
[5] B. Li, Q.W. Zhang, S.N. Mathaudhu, Scr. Mater. 134 (2017) 37–41.
[6] B. Li, P.F. Yan, M.L. Sui, E. Ma, Acta Mater. 58 (2010) 173–179.
[7] T. Obara, H. Yoshinga, S. Morozumi, Acta Metall. 21 (1973) 845–853.
[8] S.G. Song, G.T. Gray, Philos. Mag. A 71 (1995) 263–274.
[9] S.G. Song, G.T. Gray III, Acta Metall. Mater. 43 (1995) 2325–2337.
[10] S.G. Song, G.T. Gray III, Acta Metall. Mater. 43 (1995) 2339–2350.
[11] X.Y. Zhang, B. Li, Q. Liu, Acta Mater. 90 (2015) 140–150.
[12] H.D. Fan, J.A. El-Awady, J. Appl. Mech. 82 (2015) 101006.
[13] W.W. Jian, G.M. Cheng, W.Z. Xu, H. Yuan, M.H. Tsai, Q.D. Wang, C.C. Koch, Y.T. Zhu, S.N. Mathaudhu, Mater. Res. Lett. 1 (2013) 1–6.
[14] P. Cizek, M.R. Barnett, Scr. Mater. 59 (2008) 959–962.
[15] D. Ando, J. Koike, Y. Sutou, Acta Mater. 58 (2010) 4316–4324.
[16] J.W. Christian, S. Mahajan, Prog. Mater. Sci. 39 (1995) 1–157.
[17] M.R. Barnett, Mater. Sci. Eng. A 464 (2007) 8–16.
[18] X.Y. Zhang, Y.T. Zhu, Q. Liu, Scr. Mater. 63 (2010) 387–390.
[19] M.S. Daw, M.I. Baskes, Phys. Rev. Lett. 50 (1983) 1285–1288.
[20] M.S. Daw, M.I. Baskes, Phys. Rev. B 29 (1984) 6443–6453.
[21] X. Liu, J.B. Adams, F. Ercolessi, J.A. Moriarty, Model. Simul. Mater. Sci. Eng. 4 (1996) 293.
[22] M.I. Baskes, S.G. Srinivasan, S.M. Valone, R.G. Hoagland, Phys. Rev. B 75 (2007), 094113. .
[23] Z.X. Wu, W.A. Curtin, Nature 526 (2015) 62–67.
[24] A. Stukowski, Model. Simul. Mater. Sci. Eng. 18 (2010), 015012. .
[25] B. Li, E. Ma, Acta Mater. 57 (2009) 1734–1743.
[26] M. Liao, B. Li, M.F. Horstemeyer, Metall. Mater. Trans. A 45 (2014) 3661–3669.
[27] B. Li, X.Y. Zhang, Scr. Mater. 125 (2016) 73–79.
[28] B. Li, E. Ma, Phys. Rev. Lett. 103 (2009), 035503. .
[29] B.A. Bilby, A.G. Crocker, Proc. R. Soc. Lond. A Math. Phys. Sci. 288 (1965) 240–255.
[30] M. Niewczas, Acta Mater. 58 (2010) 5848–5857.
[31] A. Ostapovets, A. Serra, J. Mater. Sci. 52 (2017) 533–540.